



HHS Public Access

Author manuscript

J Enzyme Inhib Med Chem. Author manuscript; available in PMC 2015 November 29.

Published in final edited form as:

J Enzyme Inhib Med Chem. 2011 February ; 26(1): 46–55. doi:10.3109/14756361003671078.

Nantenine as an acetylcholinesterase inhibitor: SAR, enzyme kinetics and molecular modeling investigations

Stevan Pecic¹, Marie A. McAnuff², and Wayne W. Harding¹

¹City University of New York Hunter College, Department of Chemistry, 695 Park Avenue, New York, USA

²City University of New York, Hunter College, Department of Biology, 695 Park Avenue, New York, USA

Abstract

Nantenine, as well as a number of flexible analogs, were evaluated for acetylcholinesterase (AChE) inhibitory activity in microplate spectrophotometric assays based on Ellman's method. It was found that the rigid aporphine core of nantenine is an important structural requirement for its anticholinesterase activity. Nantenine showed mixed inhibition kinetics in enzyme assays. Molecular docking experiments suggest that nantenine binds preferentially to the catalytic site of AChE but is also capable of interacting with the peripheral anionic site (PAS) of the enzyme, thus accounting for its mixed inhibition profile. The aporphine core of nantenine may thus be a useful template for the design of novel PAS or dual-site AChE inhibitors. Inhibiting the PAS is desirable for prevention of aggregation of the amyloid peptide A β , a major causative factor in the progression of Alzheimer's disease (AD).

Keywords

Aporphine; AChE; alzheimer's; peripheral anionic site; ICM

Introduction

Alzheimer's disease (AD) is an incapacitating condition which afflicts millions of people worldwide. The disease is especially prevalent among the elderly and is associated with severe deficits in cognition and memory [1-3]. In the advanced stages of AD, dramatic changes in the emotional state, psychological well-being and personality are observed [4,5]. The onset and progression of AD is thought to be a consequence of the formation of neuritic plaques via aggregation of the amyloid peptide A β (the amyloid hypothesis of AD) [6-10].

Research over the years has supported early hypotheses that a deficit in cholinergic neurotransmission plays a major role in the neurodegeneration associated with the disease

Address for Correspondence: Wayne Harding, Department of Chemistry, Hunter College, CUNY, 695 Park Avenue, New York, NY 10065, USA..

Declaration of interest

The authors report no conflict of interest.

[11,12]. Acetylcholinesterase (AChE) is an enzyme which is responsible for the degradation of the neurotransmitter acetylcholine. Most of the current treatments for AD employ compounds which act as inhibitors of acetylcholinesterase and thereby improve cholinergic deficits. Four compounds are commonly prescribed for treatment of AD based on this mechanism of action namely galanthamine (**1**), tacrine (**2**), donepezil (**3**) and rivastigmine (**4**) (Figure 1) [13,14]. These therapeutics offer short-term improvement in treating symptoms of the disease with modest benefits in slowing the decline in behavior, function and cognition associated with the disease [15-17]. All of the approved AChE inhibitors have potentially serious side-effects especially with long-term use, and more efficacious and safer alternatives are desirable [18-21].

AChE has two main binding domains, the catalytic site and a peripheral anionic site (PAS) [22,23]. There is evidence that AChE facilitates the formation of amyloid fibrils via a set of amino acids located in the vicinity of the PAS and that molecules which bind to the PAS prevent aggregation of the amyloid peptide A β [24,25]. Based on these developments, there has recently emerged a new therapeutic strategy which involves the use of molecules endowed with the ability to bind to the catalytic site and PAS of AChE simultaneously [26-29]. Such dual-acting molecules should be more efficacious in decelerating the progression of the disease via prevention of A β accumulation via PAS inhibition as well as providing the usual palliative cognitive and memory improvements associated with the inhibition of the catalytic site of the enzyme.

Aporphines are a family of compounds that are structurally and biogenetically related to isoquinoline alkaloids [30]. A number of aporphines have shown biological activity as dopamine receptor and serotonin receptor ligands and there are reports of some members which have cytotoxic and antimalarial activities [31-39]. Relatively few aporphines have been evaluated as AChE inhibitors. In that regard, a recent report indicated that aporphinoids **5** and **6** (Figure 2) ex *Corydalis turtschaninovii* Besser (Papaveraceae) show moderate activity with half maximal inhibitory concentration (IC₅₀) values of 27.1 and 48.7 μ M respectively [40]. Structurally-related synthetic oxoaporphines and isooxoaporphines have been recently reported to possess anticholinesterase activity, inhibiting the enzyme non-competitively [41]. The aporphine **7** has also been reported to have moderate AChE inhibitory activity (34.5% inhibition at 10⁻⁴ M). The structural similarity between nantenine (**8**), (an aporphine which we are currently investigating as a 5-HT_{2A} receptor ligand) and the aforementioned aporphines prompted us to investigate the anticholinesterase activity of **8**. We initially compared **8** with the known AChE inhibitor galanthamine (**1**) in a TLC anticholinesterase bioautographic assay [42] and found that **8** showed activity. To understand the mode of inhibition, enzyme kinetics studies were undertaken. In order to explore the influence of molecular rigidity on AChE inhibitory activity of **8**, we have synthesised and evaluated a small library of nantenine congeners. We also performed molecular docking studies on nantenine in order to better understand its mode(s) of binding to the enzyme.

Materials and Methods

Chemistry

General Methods and Instrumentation—High resolution electron impact mass spectra (HREIMS) were obtained using an Agilent 6520 Q-TOF (Santa Clara, CA) instrument. NMR data were collected on a Bruker 500 MHz machine (Billerica, MA) with TMS as internal standard and CDCl₃ (Sigma-Aldrich Inc., St. Louis, MO) as solvent unless stated otherwise. Chemical shift (δ) values are reported in ppm and coupling constants in Hertz (Hz). Melting points were obtained on a Mel-Temp capillary electrothermal melting point apparatus. Reactions were monitored by TLC (Newark, Delaware, NJ) with Analtech Uniplate silica gel G/UV 254 (1101D, Dubuque, IA) precoated plates (0.2 mm). TLC plates were visualised by UV (254 nm) and by staining with phosphomolybdic acid reagent followed by heating. Flash column chromatography was performed with Silicagel 60 (EMD Chemicals Darmstadt, Germany, 230-400 mesh, 0.04-0.063 μ m particle size).

Synthesis

3-(benzo[d][1,3]dioxol-5-yl)-4,5-dimethoxybenzaldehyde (11): A mixture of Pd(PPh₃)₄ (2.35 g, 2.04 mmol) and commercially available 5-bromoveratraldehyde **10** (5 g, 20.4 mmol) in DME (250 mL) was stirred for 15 min at 20°C under argon. 2M aqueous K₂CO₃ (71.5 mL, 142.8 mmol) was added to the mixture, followed by boronic acid **9** (6.77 g, 40.8 mmol) in DME. The mixture was refluxed for 18 h and then cooled to RT. The reaction mixture was treated with water and ethyl acetate and the layers were separated. The organic extract was washed sequentially with 1M NaOH and water then dried over Na₂SO₄. The solvent was evaporated to give crude **10**, which was purified by column chromatography (hexanes:EtOAc, 4:1). Compound **11** (5.66 g, 96%) was obtained as a pale yellow oil: ¹H NMR (500 MHz, CDCl₃): δ 9.92 (s, 1H), 7.44 (d, 1H, *J* = 2 Hz), 7.42 (d, 1H, *J* = 2 Hz), 7.06 (d, 1H, *J* = 1.7 Hz), 7 (dd, 1H, *J* = 8, 1.7 Hz), 6.89 (d, 1H, *J* = 8 Hz), 6.02 (s, 2H), 3.97 (s, 3H); 3.71 (s, 3H); ¹³C NMR (125 MHz, CDCl₃): δ 191.2, 153.7, 151.9, 147.5, 147.2, 135.7, 132.3, 130.8, 127.2, 122.7, 109.7, 109.3, 108.3, 101.2, 60.7, 56.1. HREIMS calcd. for C₁₆H₁₄O₅ [M]⁺ 286.0841; found 286.0841.

(E)-5-(2,3-dimethoxy-5-(2-nitrovinyl)phenyl)benzo[d][1,3] dioxole (12): A mixture of aldehyde **11** (5.31 g, 18.56 mmol), ammonium acetate (1.43 g, 18.56 mmol), nitromethane (4.98 mL, 92.82 mmol), and glacial AcOH was refluxed for 4 h. After cooling to RT, the product was filtered and recrystallised from EtOH to afford **12**, as a yellow solid (5.15 g, 84%); mp 124–127°C. ¹H NMR (500 MHz, CDCl₃): δ 7.97 (d, 1H, *J* = 13.6 Hz), 7.55 (d, 1H, *J* = 13.6 Hz), 7.14 (d, 1H, *J* = 2.1 Hz), 7.02 (d, 1H, *J* = 1.7 Hz), 7.01 (d, 1H, *J* = 2.1 Hz), 6.96 (dd, 1H, *J* = 8, 1.7 Hz), 6.88 (d, 1H, *J* = 8 Hz), 6.02 (s, 2H), 3.95 (s, 3H); 3.68 (s, 3H); ¹³C NMR (125 MHz, CDCl₃): δ 153, 150.3, 147.8, 147.5, 139.2, 136.6, 136.6, 130.9, 125.9, 125.1, 122.9, 111, 109.9, 108.5, 101.4, 61, 56.3. HREIMS calcd. for C₁₇H₁₆NO₆ [M + H]⁺ 330.0899; found 330.0971.

2-(3-(benzo[d][1,3]dioxol-5-yl)-4,5-dimethoxyphenyl) ethanamine (13): trimethylsilyl chloride (TMSCl) (5 mL, 24.2 mmol) was added to a vigorously stirred suspension of LiBH₄ (0.35 g, 7.62 mmol) in anhydrous tetrahydrofuran (THF) (15 mL) over a period of 2

min. After the gas evolution had ceased, the trimethylsilane was removed by purging the solution with argon. Then, over a period of 5 min, a solution of **12** (1 g, 3.03 mmol) in anhydrous THF (15 mL) was added and the mixture was heated for 18 h at reflux. After cooling to RT, the mixture was quenched carefully with methanol (25 mL) at 0°C. The solvent was removed with a rotatory evaporator, the resulting residue dissolved in 20% aq KOH (50 mL), and extracted with DCM (3 × 50 mL). The combined extracts were dried (Na₂SO₄) and then concentrated under reduced pressure. This gave **13** as an oil (0.90 g, 99%). ¹H NMR (500 MHz, CDCl₃): δ 7.1 (d, 1H, *J* = 1.3 Hz), 7.04 (d, 1H, *J* = 1.5, 8 Hz), 6.88 (d, 1H, *J* = 8 Hz), 6.77 (s, 1H), 6.76 (s, 1H), 6.02 (s, 2H), 3.92 (s, 3H), 3.62 (s, 3H), 3.01 (t, 2H, *J* = 7 Hz), 2.75 (t, 2H, *J* = 7 Hz). ¹³C NMR (125 MHz, CDCl₃): δ 153, 147.3, 146.7, 144.8, 135.7, 135.2, 132.2, 122.6, 122.6, 111.9, 109.9, 108.1, 101, 60.5, 56, 43.5, 40.

N-(3-(benzo[d][1,3]dioxol-5-yl)-4,5-dimethoxyphenethyl) formamide (14a): Amine **13** (0.46 g, 1.53 mmol), ethyl formate (0.31 mL, 3.9 mmol) and triethylamine (0.43 mL, 3.10 mmol) were heated to reflux for 48 h. Removal of excess ethyl formate and triethylamine under reduced pressure gave a dark-brown oil, that was purified by column chromatography (MeOH:DCM, 1:99). Compound **14a** (0.46 g, 90.8%) was obtained as an orange-red oil: ¹H NMR (500 MHz, CDCl₃): δ 8.12 (s, 1H), 7.05 (s, 1H), 6.98 (d, 1H, *J* = 8 Hz), 6.85 (d, 1H, *J* = 8 Hz), 6.73 (br. s, 2H), 5.98 (s, 2H), 3.88 (s, 3H), 3.56 (m, 6H), 2.82 (t, 2H, *J* = 6.9 Hz); ¹³C NMR (125 MHz, CDCl₃): δ 161.4, 153.1, 147.4, 146.8, 135.4, 134.4, 133.6, 131.9, 122.7, 122.6, 111.7, 109.9, 108.2, 101.2, 60.6, 56.1, 39.3, 35.5. HREIMS calcd. for C₁₈H₂₀NO₅ [M+H]⁺ 330.1263; found 330.1333.

N-(3-(benzo[d][1,3]dioxol-5-yl)-4,5-dimethoxyphenethyl) acetamide (14b): The amine **13** (0.32 g, 1.06 mmol), acetyl chloride (0.12 mL, 5.5 mmol) and triethylamine (0.45 mL, 10 mmol) were mixed with dichloromethane (10 mL) and stirred for 6 hours at 0°C. The reaction was treated with saturated sodium bicarbonate, extracted with DCM (3 × 35 mL), dried over Na₂SO₄ and concentrated under reduced pressure to give a yellow oil, that was subsequently purified by column chromatography (MeOH:DCM, 1:99). Compound **14b** (0.33 g, 91%) was obtained as an orange-red oil: ¹H NMR (500 MHz, CDCl₃): δ 8.12 (s, 1H), 7.06 (br. s, 1H), 6.98 (d, 1H, *J* = 8 Hz), 6.86 (d, 1H, *J* = 8 Hz), 6.73 (br. s, 1H), 5.98 (s, 2H), 5.71 (br. s, 1H), 3.88 (s, 3H), 3.58 (s, 3H), 3.51 (dd, 2H, *J* = 13.2, 6.5 Hz), 2.78 (t, 2H, *J* = 7 Hz), 1.95 (s, 3H); ¹³C NMR (125 MHz, CDCl₃): δ 170.1, 153.1, 147.4, 146.8, 145, 135.4, 134.7, 131.9, 122.6, 122.5, 111.7, 109.8, 108.1, 101, 60.5, 56, 40.7, 35.6, 23.4. HREIMS calcd. for C₁₉H₂₂NO₅ [M+H]⁺ 344.1415; found 344.1488.

Synthesis of compounds 15a and 15b: To a stirred solution of amide **14a** (0.46 g, 1.4 mmol) in acetonitrile (5 mL) was added POCl₃ (0.65 mL, 7 mmol) at RT, and the resulting mixture was heated at 50°C for 12 h. The reaction mixture was concentrated, and the quaternary salt was dissolved in DCM (25 mL). After the mixture was cooled to 0°C, it was diluted with water, made basic with 5% aqueous NH₄OH, and extracted with DCM (3 × 25 mL). The organic solution was washed with water (30 mL), dried with anhydrous Na₂SO₄ and concentrated to give a yellow crude dihydroisoquinoline. Sodium borohydride (1.04 g, 27.6 mmol) was added portion-wise to a stirred solution of the crude dihydroisoquinoline in methanol (20 mL) and the mixture was stirred at 0°C for 3 h. The reaction mixture was

concentrated, and excess NaBH₄ was destroyed by adding water and glacial acetic acid until gas evolution ceased. The mixture was extracted with DCM (3 × 25 mL), dried over Na₂SO₄ and concentrated to give orange oil. This crude oily tetrahydroisoquinoline was treated with aqueous formaldehyde solution, (37%, 2.59 mL, 2.55 mmol) in anhydrous DCM (10 mL) and then with NaBH(OAc)₃ (1.35 g, 6.38 mmol). The mixture was allowed to stir at RT for 24 h. The reaction was quenched with 5% aqueous sodium bicarbonate (25 mL), and extracted with ethyl acetate (2 × 25 mL), dried over Na₂SO₄ and concentrated to dryness. The residue was purified via silica flash column chromatography (MeOH:DCM, 2:98) to provide **15a**. Similar procedures were used to prepare **15b** from **14b**.

8-(benzo[d][1,3]dioxol-5-yl)-6,7-dimethoxy-2-methyl-1,2,3,4-tetrahydroisoquinoline (15a): **15a** was prepared from **14a** in 88% overall yield as bright yellow crystals: mp 82–84°C. ¹H NMR (500 MHz, CDCl₃): δ 6.87 (d, 1H, *J* = 7.9 Hz), 6.70–6.65 (m, 3H), 6.01 (d, 2H, *J* = 8.4 Hz), 3.88 (s, 3H), 3.54 (s, 3H), 3.15 (br. s, 2H), 2.94 (br. s, 2H), 2.65 (br. s, 2H), 2.35 (s, 3H); ¹³C NMR (125 MHz, CDCl₃): δ 151, 147.3, 146.5, 144.8, 134, 129.8, 129.5, 125.8, 122.6, 111.6, 110, 108.2, 101, 60.8, 56.5, 55.8, 52.6, 46.3, 29.8; HREIMS calcd. for C₁₉H₂₁NO₄ [M]⁺ 327.1478; found 327.1471.

8-(benzo[d][1,3]dioxol-5-yl)-6,7-dimethoxy-1,2-dimethyl-1,2,3,4-tetrahydroisoquinoline (15b): Prepared from **14b**, as a mixture of isomers, in 90% overall yield as bright yellow crystals: mp 101–104°C. ¹H NMR (500 MHz, CDCl₃): δ 6.87–6.84 (m, 1H), 6.76–6.67 (m, 1H), 6.66–6.65 (m, 2H), 6.03–6 (m, 2H), 3.87 (s, 3H), 3.78–3.71 (m, 1H), 3.53–3.49 (m, 3H), 3.08–3.07 (m, 2H), 2.77–2.71 (m, 2H), 2.38–2.46 (m, 3H), 0.97–0.94 (m, 3H); ¹³C NMR (125 MHz, CDCl₃) (doubling of signals observed; average values for isomeric shifts reported): δ 151, 147.3, 146.5, 145.1, 134.6, 130.8, 129.9, 128.6, 123.3, 112, 110.6, 108.1, 101, 60.8, 55.7, 55, 44.1, 42, 26.3, 16.2; HREIMS calcd. for C₂₀H₂₃NO₄ [M]⁺ 341.1627; found 341.1628.

AChE Inhibition Assays

AChE inhibition was determined using the method of Adsersen et al [43] with ATCI as substrate. In brief, to a 96-well microplate, 25 μL substrate, 15mM ATCI in water, 125 μL 3 mM DTNB in buffer C (50 mM Tris–HCl, pH 8, 0.1M NaCl, 0.02 M MgCl₂·6H₂O), 72.5 μL buffer B (50 mM Tris–HCl, pH 8, 0.1% bovine serum albumin) and 2.5 μL test compound solution dissolved in DMSO were added and the absorbance was measured seven times at 405 nm every 19 s in a PowerWave 200 Microplate Scanning Spectrophotometer (Winooski, VT). Then 25 μL AChE (0.22 U/mL in buffer B) was added to each of the wells and the absorbance was measured again seven times at 405 nm every 19 s. The reaction rate was calculated by the GraphPad Prism software version 5.0 (LaJolla, CA) and Microsoft Excel. Any increase in absorbance due to the spontaneous hydrolysis of substrate was corrected by subtracting the rate of the reaction before adding the enzyme. Percentage inhibition was calculated by comparing the rates for the samples to the blank (2.5 μL DMSO instead of test compound solution). IC₅₀ values were calculated by nonlinear regression analysis using GraphPad Prism. Each experiment was performed in triplicate [43].

Docking studies with Nantenine

The binding of the nantenine and *Electrophorus electricus* AChE was examined *in silico*. All docking studies were performed using Internal Coordinate Mechanics (Molsoft ICM version 3.6-1, LaJolla, CA) package. The ICM score considers several free energy terms such as van der Waals, hydrogen bonding, Poisson electrostatic desolvation and entropy. ICM sequence-structure alignment is based on zero end gap global alignment (ZEGA) sequence alignment [44] (Needleman and Wunsch algorithm with zero gap and penalties).

Preparation of Homology Model

Since a high-resolution crystal structure of *E. electricus* AChE is not available, the homology model for molecular modeling purposes was built based on the X-ray crystal structure of *Torpedo californica* AChE in complex with bis-(5)-tacrine (PDB code 2CMF) which was obtained from the Protein Data Bank. The tacrine ligand and water molecules present in the pdb file were removed prior to building the model. The sequence of *E. electricus* AChE was aligned with the sequence of *Torpedo californica* AChE, and showed 70% identity. For the sequence alignment step, the following parameters were used:

Alignment Algorithm: ZEGA

Gap Open: 2.4

Gap Extension: 0.15

maxPenalizedGap: 99

This alignment, along with a file containing the atomic coordinates of *Torpedo californica* AChE, was used as an input to the ICM PRO software package to generate the homology model. For the homology model building step the following parameters were used:

3D template: 2CMF

Max loop length: 100

Nterm extension: 1

Cterm extension: 1

Expand gaps by: 1

After energy-minimising using ICM-PRO, the receptor model was saved and used for docking studies.

Generation of ligands—The 2D structure of nantenine (or analogs **15a**, **15b**, **16** and **17**) was drawn with ChemDraw Ultra version 9.0 (Cambridge, MA) and energy minimised through Chem3D Ultra version 9.0/MOPAC (Cambridge, MA), Job Type: Minimum RMS Gradient of 0.01 kcal/mol and RMS distance of 0.1 Å, and saved as MDL MolFile (*.mol).

Docking using the Molsoft ICM 3.6-1 program [45]—To perform the ICM small molecule docking the following steps were executed according to the program guidelines:

- (1) Setup docking project:

- (i) The project name was set.
 - (ii) The enzyme (receptor) was setup: (The receptor molecule was entered in the receptor molecule data entry box, the binding sites were identified by clicking on the “identify binding sites” button. In this way potential ligand binding pockets were identified. After the receptor setup was complete, the program displayed the receptor with selected binding site residues highlighted in yellow x-7stick presentation).
 - (iii) The binding site was reviewed and adjusted: ICM made a box around the ligand binding site based on the information entered in the receptor setup section. The position of the box encompassed the residues expected to be involved in ligand binding.
 - (iv) Receptor maps were made: Energy maps of the environment within the docking box were constructed. Flexibility of the receptor residues was set to 4.0.
- (2) Docking simulation was executed: Interactive docking was used to dock nantenine and the other analogs. The molecules were docked in non-chiral mode. The thoroughness level was set to the maximum value of 10. ICM scores were obtained after this procedure.

Results

Chemistry

Compounds **15a** and **15b** were prepared as outlined in Scheme 1. Commercially available boronic acid **9** and bromoaldehyde **10** were coupled under Suzuki conditions [46,47] affording the biaryl intermediate (**11**). A nitro-aldol reaction [48,49] on **11** followed by reduction of the nitrostyrene (**12**), gave amine **13**. Compound **13** was condensed with ethyl formate or with acetyl chloride to give amides **14a** and **14b**. These amides were then subjected to Bischler-Napieralski [50,51] cyclisation to afford intermediate dihydroisoquinolines which were immediately reduced with NaBH₄ to give intermediate tetrahydroisoquinoline products (due to instability of the imines). Methylation of the tetrahydroisoquinoline intermediates under reductive-amination conditions then furnished the target *seco*-ring C derivatives **15a** and **15b**. Compounds **16** and **17** (Figure 3) were prepared as reported by us elsewhere [52].

Enzyme inhibition and kinetics assays

IC₅₀ values for compounds **8**, **15a**, **15b**, **16** and **17** determined with a microplate assay [53] using lyophilised *Electrophorus electricus* AChE (Type VI, Sigma-Aldrich, MO) and based on Ellman's method, are summarised in Table 1. The lead compound nantenine, showed the highest inhibitory activity with an IC₅₀ of 1.09 μM. The *seco*-ring C analogs **15a** and **15b** were prepared to evaluate whether the rigid aporphine frame-work was required for activity. We were also interested in evaluating these compounds since they are more accessible synthetically, so that any follow-up SAR studies would be facilitated. Both compounds were

approximately two-fold less active than nantenine. Compound **16**, in which the biaryl bond of nantenine is absent, was 17 times less active than the lead molecule. The flexible analog **17** had the lowest inhibitory activity among the ring-truncated analogs, being inactive ($IC_{50} > 100 \mu M$). Taking together the results obtained from the SAR analysis of this set of compounds, it is apparent that ring C and ring B are required to be intact for anticholinesterase activity. Therefore it appears that the rigid aporphine core of nantenine is an important structural feature for AChE inhibitory activity.

To determine the mode of inhibition exhibited by nantenine, we carried out an evaluation of the steady-state kinetics of the enzyme in the presence of nantenine. A double reciprocal ($1/V$ vs $1/[S]$, Lineweaver-Burk) plot was performed and this indicated mixed inhibition since lines of increasing gradient showed increasing x-intercepts (Figure 4). Figure 5 shows a Dixon plot which allowed for calculation of the K_i of nantenine in this assay ($18.7 \mu M$).

Docking experiments

To further understand the structural basis for the anti-AChE activity seen in **8**, molecular docking experiments were performed with the program ICM Pro[®] [54]. The crystal structure of *Torpedo californica* AChE (*TcAChE*) bound to bis-(5)-tacrine was obtained from the Protein Data Bank (PDB) - PDB code 2CMF. Bis-(5)-tacrine was removed and a homology model was generated for *Electrophorus electricus* AChE using the homology modeling features of the program. Manipulations were performed to allow for identification of the binding sites in the homology modelled enzyme. After energy-minimisation, nantenine was docked into the identified binding regions of the enzyme. Scoring functions from this docking experiment are reported in Table 2. The known catalytic site inhibitor galanthamine (**1**) was also docked for comparison. The docking scores suggest that nantenine may bind preferentially to the catalytic site since the three most favorable conformations are located in this site.

Catalytic site interactions of nantenine—Inspection of the top binding pose in the active site indicates that nantenine interacts with the enzyme via π - π stacking interactions between the Trp84 and rings A and D as well as similar interactions between the Tyr330 and ring D. Both of these interactions occur in the anionic sub-site [55] region of the enzyme. Of the three amino acid residues in the catalytic triad [56] (His440, Ser200 and Glu327), nantenine interacts only with Ser 200 (via the hydrophobic contacts with ring B). Nantenine also shows interactions with Gly118 in the oxyanion hole [57] region of AChE. Other hydrophobic interactions help to stabilise the molecule in the active site. Interactions of nantenine in the catalytic site of the enzyme have been displayed with LigPlot [58] (Figure 6) for ease of viewing.

PAS interactions of nantenine—The ICM docking experiments also predicted binding poses for nantenine in the PAS. Figure 7 shows a LigPlot model for the key interactions of pose number four which indicates that nantenine is stabilised via a hydrogen-bonding interaction between the C2 oxygen atom and the phenolic group of Tyr70 in the PAS. π - π stacking interactions between the aromatic rings of nantenine and Trp279 as well as between

Y334 and ring A also seems to be important for binding to the PAS, based on inspection of our ICM model.

The ICM models may be used to explain the mode of inhibition exhibited by nantenine; The mixed mode of inhibition is most likely to be due to nantenine binding to both the catalytic site and PAS.

Docking of 15a, 16 and 17—In order to begin to rationalise the trends in anticholinesterase activity seen in our analogs, ICM docking simulations were then performed with compounds **15a**, **16** and **17**. Table 3 summarises results from these docking experiments. The docked poses were evaluated by visual inspection. The three lowest energy poses for compound **15a** were all located in the catalytic site.

However, in the case of compound **16**, among the top three binding poses, one was in the PAS, one in the catalytic site and the third in both the catalytic site and PAS. Compound **17** did not dock into the catalytic site or the PAS of the enzyme which is consistent with the low activity observed with this compound (Table 1). Visual inspection showed that compound **17** was docked in a region on the outer surface of the enzyme. Therefore, the relatively good ICM score obtained for compound **17** is clearly not due to the active site or PAS inhibition.

Discussion

Alzheimer's disease (AD) is a neurodegenerative condition, the onset and progression of which is associated with deficits in cholinergic neurotransmission as well as aggregation of the amyloid peptide A β [6-10]. A major biological target for the development of anti-AD drugs is the enzyme acetylcholinesterase. Inhibitors of acetylcholinesterase have proved to be of therapeutic value in the treatment of Alzheimer's disease and have been the front-line approach in this regard [13,14]. This enzyme is known to possess two binding domains: a catalytic site which binds the endogenous neurotransmitter acetylcholine and catalyses its degradation and a peripheral anionic site [22,23]. Clinically available inhibitors have the inhibition of the catalytic site of the enzyme as an integral part of their mode of action. This mode of action of anti-AD drugs is in line with the cholinergic hypothesis of Alzheimer's disease [59,60]. However, current interest is in the identification and development of molecules which potentially inhibit both the catalytic site and peripheral anionic site of the enzyme [27]. Dual-site inhibition of the enzyme is beneficial, since inhibition of the catalytic site results in improvements in cholinergic deficits, while inhibition of the peripheral anionic site prevents aggregation of toxic amyloid peptide A β [24,25,61]. A number of chemical scaffolds have been identified which fit this role, some of which utilise a dimeric design for dual AChE inhibition [62-64]. Our work here indicates that the aporphine scaffold may represent another opportunity to develop novel dual-site AChE inhibitors.

A number of analogues of our lead molecule, nantenine were synthesised and evaluated in an Ellman assay for AChE inhibition. These analogs were designed to probe the requirements for structural rigidity of the aporphine core of the lead compound in inhibiting

the enzyme. We found that the rigidity of nantenine was an important structural feature for AChE inhibition. Others have found that the less rigid tetrahydroisoqui-noline precursors of some aporphines show higher levels of AChE inhibition than the aporphines [65]. These results together suggest that the structural rigidity of aporphines as a group per se is not the only determinant of enzyme activity, although in the case of nantenine this rigidity does appear to play a significant role. Nantenine showed mixed inhibition kinetics in our enzyme assays. Interestingly, nantenine was previously shown to be inactive in an AChE assay with rat synaptosomal membrane as the enzyme source [66]. The assay conditions or source of the enzyme may account for the discrepancy in both the previous and currently reported results.

Our docking experiments suggest that nantenine is capable of binding to both the catalytic site and the PAS of AChE, which could account for its mixed mode of inhibition. This study is the first to examine the docking of aporphines and the flexible analogs, although there is one recent study where the docking of structurally related oxoaporphines and oxoisoaporphines was reported [67]. Like nantenine, the molecular modelling experiments suggest that the oxoaporphines and oxoisoaporphines interact with the PAS. In the case of the flexible analogs **15a**, **16** and **17**, we found that visual inspection of the docked ICM poses seems to be a good method for predicting activity or lack thereof in this series of compounds. However, the top three ICM scores for nantenine (**8**), **15a** and **16** did not show good qualitative correlation with the observed inhibitory activities, suggesting that the ICM score is not a good predictor of relative AChE inhibitory activity for this series. This may be due in part to the occurrence of multiple binding modes for these compounds.

In considering the design of novel anti-AD drugs, dual inhibition of AChE is a significant strategy to explore. Nantenine is an interesting lead for such studies. Apart from the dual inhibitory profile, pharmacokinetic factors such as blood-brain barrier penetrability will also be important in the future design of potential anti-AD nantenine analogs. The optimal clogP for blood-brain barrier penetrability is 2–5 [68]. In this regard, nantenine is perhaps a better lead than some other anti-AChE aporphinoids previously identified such as compound **5** [40], which predictably will not cross the blood-brain barrier due to its quaternised nitrogen functionality (clogP of nantenine and **5** = 3.6 and –1.4 respectively as calculated with ChemBioDraw Ultra version 11).

Conclusions

SAR explorations have revealed that the rigid structure of nantenine is important for anticholinesterase activity; increasing molecular flexibility was associated with a decrease in AChE inhibition. Since the inhibition was of the mixed type, it is perceptible that nantenine binds to both the PAS and the catalytic site. This is corroborated by our molecular docking studies which indicated key H-bond and π - π stacking interactions of nantenine in the PAS. The aporphine scaffold of nantenine may be useful for the synthesis of novel PAS or dual-site AChE inhibitors.

References

1. Corey-Bloom J. The ABC of Alzheimer's disease: cognitive changes and their management in Alzheimer's disease and related dementias. *Int Psychogeriatr.* 2002; 14:51–75. [PubMed: 12636180]
2. Akhondzadeh S, Noroozian M. Alzheimer's disease: pathophysiology and pharmacotherapy. *IDrugs.* 2002; 5:1062–1069. [PubMed: 12800059]
3. Backman L, Jones S, Berger AK, Laukka EJ, Small BJ. Cognitive impairment in preclinical Alzheimer's disease: a meta-analysis. *Neuropsychology.* 2005; 19:520–531. [PubMed: 16060827]
4. Shimokawa A, Yatomi N, Anamizu S, Torii S, Isono H, Sugai Y, Kohno M. Influence of deteriorating ability of emotional comprehension on interpersonal behavior in Alzheimer-type dementia. *Brain Cognition.* 2001; 47:423–433. [PubMed: 11748898]
5. Weinshenker D. Functional consequences of locus coeruleus degeneration in Alzheimer's disease. *Curr Alzheimer Res.* 2008; 5:342–345. [PubMed: 18537547]
6. Hardy J. Alzheimer's disease: the amyloid cascade hypothesis: an update and reappraisal. *J Alzheimers Dis.* 2006; 9:151–153. [PubMed: 16914853]
7. Pimplikar SW. Reassessing the amyloid cascade hypothesis of Alzheimer's disease. *Int J Biochem Cell B.* 2009; 4:1261–1268.
8. Korczyn AD. The amyloid cascade hypothesis. *Alzheimers Dement.* 2008; 4:176–178. [PubMed: 18631966]
9. Eckman CB, Eckman EA. An update on the amyloid hypothesis. *Neurol Clin.* 2007; 25:669–682. [PubMed: 17659184]
10. Hardy JA, Higgins GA. Alzheimer's disease: the amyloid cascade hypothesis. *Science.* 1992; 256:184–185. [PubMed: 1566067]
11. Sivaprakasam K. Towards a unifying hypothesis of Alzheimer's disease: cholinergic system linked to plaques, tangles and neuroinflammation. *Curr Med Chem.* 2006; 13:2179–2188. [PubMed: 16918347]
12. Terry AV Jr, Buccafusco JJ. The cholinergic hypothesis of age and Alzheimer's disease-related cognitive deficits: recent challenges and their implications for novel drug development. *J Pharmacol Exp Ther.* 2003; 306:821–827. [PubMed: 12805474]
13. Sabbagh MN, Farlow MR, Relkin N, Beach TG. Do cholinergic therapies have disease-modifying effects in Alzheimer's disease? *Alzheimers Dement.* 2006; 2:118–125. [PubMed: 19595868]
14. Colombres M, Sagal JP, Inestrosa NC. An overview of the current and novel drugs for Alzheimer's disease with particular reference to anti-cholinesterase compounds. *Curr Pharm Design.* 2004; 10:3121–3130.
15. Hansen RA, Gartlehner G, Webb AP, Morgan LC, Moore CG, Jonas DE. Efficacy and safety of donepezil, galantamine, and rivastigmine for the treatment of Alzheimer's disease: a systematic review and meta-analysis. *Clin Interv Aging.* 2008; 3:211–225. [PubMed: 18686744]
16. Ritchie CW, Ames D, Clayton T, Lai R. Metaanalysis of randomized trials of the efficacy and safety of donepezil, galantamine, and rivastigmine for the treatment of Alzheimer disease. *Am J Geriatr Psychiatry.* 2004; 12:358–369. [PubMed: 15249273]
17. Wagstaff AJ, McTavish D. Tacrine. A review of its pharmacodynamic and pharmacokinetic properties, and therapeutic efficacy in Alzheimer's disease. *Drugs Aging.* 1994; 4:510–540. [PubMed: 7521234]
18. Loy C, Schneider L. Galantamine for Alzheimer's disease and mild cognitive impairment. *Cochrane database of systematic reviews (Online).* 2006; (1):CD001747.
19. Heinze M, Andrae D, Grohmann R. Rivastigmin and impaired motor function. *Pharmacopsychiatry.* 2002; 35:79–80. [PubMed: 11951151]
20. Dunn NR, Pearce GL, Shakir SA. Adverse effects associated with the use of donepezil in general practice in England. *J Psychofarmacol.* 2000; 14:406–408. [PubMed: 11198060]
21. Moller HJ. Reappraising neurotransmitter-based strategies. *Eur Neuro-psychopharmacol.* 1999; 9:S53–9.

22. Bolognesi ML, Minarini A, Rosini M, Tumiatti V, Melchiorre C. From dual binding site acetylcholinesterase inhibitors to multi-target-directed ligands (MTDLs): a step forward in the treatment of Alzheimer's disease. *Mini-Rev Med Chem*. 2008; 8:960–967. [PubMed: 18782050]
23. Cavalli A, Bottegoni G, Raco C, De Vivo M, Recanatini M. A computational study of the binding of propidium to the peripheral anionic site of human acetylcholinesterase. *J Med Chem*. 2004; 47:3991–3999. [PubMed: 15267237]
24. Inestrosa NC, Sagal JP, Colombres M. Acetylcholinesterase interaction with Alzheimer amyloid beta. *Sub-cell Biochem*. 2005; 38:299–317.
25. De Ferrari GV, Canales MA, Shin I, Weiner LM, Silman I, Inestrosa NC. A structural motif of acetylcholinesterase that promotes amyloid beta-peptide fibril formation. *Biochemistry*. 2001; 40:10447–10457. [PubMed: 11523986]
26. Bolognesi ML, Cavalli A, Valgimigli L, Bartolini M, Rosini M, Andrisano V, Recanatini M, Melchiorre C. Multi-target-directed drug design strategy: from a dual binding site acetylcholinesterase inhibitor to a trifunctional compound against Alzheimer's disease. *J Med Chem*. 2007; 50:6446–6449. [PubMed: 18047264]
27. del Monte-Millan M, Garcia-Palmero E, Valenzuela R, Usan P, de Austria C, Munoz-Ruiz P, Rubio L, Dorronsoro I, Martinez A, Medina M. Dual binding site acetylcholinesterase inhibitors: potential new disease-modifying agents for AD. *J Mol Neurosci*. 2006; 30:85–88. [PubMed: 17192640]
28. Munoz-Ruiz P, Rubio L, Garcia-Palmero E, Dorronsoro I, del Monte-Millan M, Valenzuela R, et al. Design, synthesis, and biological evaluation of dual binding site acetylcholinesterase inhibitors: new disease-modifying agents for Alzheimer's disease. *J Med Chem*. 2005; 48:7223–7233. [PubMed: 16279781]
29. Camps P, Formosa X, Munoz-Torrero D, Petrignet J, Badia A, Clos MV. Synthesis and pharmacological evaluation of huprine-tacrine heterodimers: subnanomolar dual binding site acetylcholinesterase inhibitors. *J Med Chem*. 2005; 48:1701–1704. [PubMed: 15771413]
30. Shamma M, Guinaudeau H. Biogenetic pathways for the aporphinoid alkaloids. *Tetrahedron*. 1984; 40:4795–4822.
31. Si YG, Gardner MP, Tarazi FI, Baldessarini RJ, Neumeyer JL. Synthesis and binding studies of 2-O- and 11-O-substituted N-alkylnoraporphines. *Bioorg Med Chem Lett*. 2008; 18:3971–3973. [PubMed: 18585036]
32. Si YG, Gardner MP, Tarazi FI, Baldessarini RJ, Neumeyer JL. R(-)-N-alkyl-11-hydroxy-10-hydroxymethyl- and 10-methyl-aporphines as 5-HT1A receptor ligands. *Bioorg Med Chem Lett*. 2007; 17:4128–4130. [PubMed: 17543523]
33. Toth M, Berenyi S, Csutoras C, Kula NS, Zhang K, Baldessarini RJ, Neumeyer JL. Synthesis and dopamine receptor binding of sulfur-containing aporphines. *Bioorg Med Chem*. 2006; 14:1918–1923. [PubMed: 16290940]
34. Hedberg MH, Linnanen T, Jansen JM, Nordvall G, Hjorth S, Unelius L, et al. 11-substituted (R)-aporphines: synthesis, pharmacology, and modeling of D2A and 5-HT1A receptor interactions. *J Med Chem*. 1996; 39:3503–3513. [PubMed: 8784448]
35. Kula NS, Baldessarini RJ, Keabian JW, Neumeyer JL. S-(+)-aporphines are not selective for human D3 dopamine receptors. *Cell Mol Neurobiol*. 1994; 14:185–191. [PubMed: 7842476]
36. Cannon JG, Jackson H, Long JP, Leonard P, Bhatnagar RK. 5-HT1A-receptor antagonism: N-alkyl derivatives of (R)-(-)-8,11-dimethoxynoraporphine. *J Med Chem*. 1989; 32:1959–1962. [PubMed: 2569041]
37. Neumeyer JL, Arana GW, Law SJ, Lamont JS, Kula NS, Baldessarini RJ. Aporphines, 36. Dopamine receptor interactions of trihydroxyaporphines. Synthesis, radioreceptor binding, and striatal adenylate cyclase stimulation of 2,10,11-trihydroxyaporphines in comparison with other hydroxylated aporphines. *J Med Chem*. 1981; 24:1440–1445. [PubMed: 7310821]
38. Likhitwitayawuid K, Angerhofer CK, Chai H, Pezzuto JM, Cordell GA, Ruangrunsi N. Cytotoxic and antimalarial alkaloids from the tubers of *Stephania pierrei*. *J Nat Prod*. 1993; 56:1468–1478. [PubMed: 8254346]

39. Chaudhary S, Pecic S, Le Gendre O, Harding WW. Microwave-assisted direct biaryl coupling: first application to the synthesis of aporphines. *Tetrahedron Lett.* 2009; 50:2437–2439. [PubMed: 20161231]
40. Hung TM, Na M, Dat NT, Ngoc TM, Youn U, Kim HJ, et al. Cholinesterase inhibitory and anti-amnesic activity of alkaloids from *Corydalis turtschaninovii*. *J Ethnopharmacol.* 2008; 119:74–80. [PubMed: 18601993]
41. Tang H, Wei YB, Zhang C, Ning FX, Qiao W, Huang SL, et al. Synthesis, biological evaluation and molecular modeling of oxoisoaporphine and oxoaporphine derivatives as new dual inhibitors of acetylcholinesterase/butrylcholinesterase. *Eur J Med Chem.* 2009; 44:2523–2532. [PubMed: 19243862]
42. Marston A, Kissling J, Hostettmann K. A rapid TLC bioautographic method for the detection of acetylcholinesterase and butrylcholinesterase inhibitors in plants. *Phytochem Anal.* 2002; 13:515–4.
43. Adersen A, Kjolbye A, Dall O, Jager AK. Acetylcholinesterase and butrylcholinesterase inhibitory compounds from *Corydalis cava* Schweigg. *Kort. J Ethnopharmacol.* 2007; 113:179–182. [PubMed: 17574358]
44. Abagyan RA, Batalov S. Do aligned sequences share the same fold? *J Mol Biol.* 1997; 273:355–368. [PubMed: 9367768]
45. Farag NA, Mohamed SR, Soliman GA. Design, synthesis, and docking studies of novel benzopyrone derivatives as H(1)-antihistaminic agents. *Bioorg Med Chem.* 2008; 16:9009–9017. [PubMed: 18789706]
46. Shrestha S, Bhattarai BR, Kafle B, Lee K-H, Cho H. Derivatives of 1,4-bis(3-hydroxycarbonyl-4-hydroxyl)styrylbenzene as PTP1B inhibitors with hypoglycemic activity. *Bioorg Med Chem.* 2008; 16:8643–8652. [PubMed: 18722777]
47. Suzuki, A. The Suzuki reaction with arylboron compounds in arene chemistry. In: Suzuki, A., editor. *Modern Arene Chemistry*. Wiley-VCH; New York: 2002. p. 53-106.
48. Yasuhara T, Zaima N, Hashimoto S, Yamazaki M, Muraoka O. First total synthesis of crispine B by nitro aldol and the Bischler-Napieralski reaction. *Heterocycles.* 2009; 77:1397–1402.
49. Hynes PS, Stupp PA, Dixon DJ. Organocatalytic Asymmetric Total Synthesis of (R)-Rolipram and Formal Synthesis of (3S,4R)-Paroxetine. *Org Lett.* 2008; 10:1389–1391. [PubMed: 18324820]
50. Liermann JC, Opatz T. Synthesis of lamellarin U and lamellarin G trimethyl ether by alkylation of a deprotonated alpha-aminonitrile. *J Org Chem.* 2008; 73:4526–4531. [PubMed: 18500839]
51. Wang YC, Georghiou PE. First enantioselective total synthesis of (–)-tejedine. *Org Lett.* 2002; 4:2675–2678. [PubMed: 12153207]
52. Chaudhary S, Pecic S, Legendre O, Navarro HA, Harding WW. (+/-)-Nantenine analogs as antagonists at human 5-HT(2A) receptors: C1 and flexible congeners. *Bioorg Med Chem Lett.* 2009; 19:2530–2532. [PubMed: 19328689]
53. Rhee IK, van de Meent M, Ingkaninan K, Verpoorte R. Screening for acetylcholinesterase inhibitors from Amaryllidaceae using silica gel thin-layer chromatography in combination with bioactivity staining. *J Chromatogr.* 2001; 915:217–223.
54. Cardozo T, Totrov M, Abagyan R. Homology modeling by the ICM method. *Proteins: Structure, Function, and Genetics.* 1995; 23:403–414.
55. Szegletes T, Mallender WD, Rosenberry TL. Nonequilibrium analysis alters the mechanistic interpretation of inhibition of acetylcholinesterase by peripheral site ligands. *Biochemistry.* 1998; 37:4206–4216. [PubMed: 9521743]
56. Sussman JL, Harel M, Frolow F, Oefner C, Goldman A, Toker L, et al. Atomic structure of acetylcholinesterase from *Torpedo californica*: a prototypic acetylcholine-binding protein. *Science.* 1991; 253:872–879. [PubMed: 1678899]
57. Harel M, Quinn DM, Nair HK, Silman I, Sussman JL. The x-ray structure of a transition state analog complex reveals the molecular origins of the catalytic power and substrate specificity of acetylcholinesterase. *J Am Chem Soc.* 1996; 118:2340–2346.
58. Wallace AC, Laskowski RA, Thornton JM. LIGPLOT: a program to generate schematic diagrams of protein-ligand interactions. *Protein Eng.* 1995; 8:127–134. [PubMed: 7630882]

59. Perry EK. The cholinergic hypothesis—ten years on. *Br Med Bull.* 1986; 42:63–69. [PubMed: 3513895]
60. Bartus RT, Dean RL, Pontecorvo MJ, Flicker C. The cholinergic hypothesis: a historical overview, current perspective, and future directions. *Ann N Y Acad Sci.* 1985; 444:332–358. [PubMed: 2990293]
61. Holzgrabe U, Kapkova P, Alptuzun V, Scheiber J, Kugelmann E. Targeting acetylcholinesterase to treat neurodegeneration. *Expert Opin Ther Targets.* 2007; 11:161–179. [PubMed: 17227232]
62. Shen Y, Zhang J, Sheng R, Dong X, He Q, Yang B, et al. Synthesis and biological evaluation of novel flavonoid derivatives as dual binding acetylcholinesterase inhibitors. *J Enzyme Inhib Med Chem.* 2009; 24:372–380. [PubMed: 18830885]
63. Haviv H, Wong DM, Silman I, Sussman JL. Bivalent ligands derived from Huperzine A as acetylcholinesterase inhibitors. *Curr Top Med Chem.* 2007; 7:375–387. [PubMed: 17305579]
64. Dorronsoro I, Alonso D, Castro A, del Monte M, Garcia-Palomero E, Martinez A. Synthesis and biological evaluation of tacrine-thiadiazolidinone hybrids as dual acetylcholinesterase inhibitors. *Arch Pharm (Weinheim).* 2005; 338:18–23. [PubMed: 15674800]
65. Markmee S, Ruchirawat S, Prachyawarakorn V, Ingkaninan K, Khorana N. Isoquinoline derivatives as potential acetylcholinesterase inhibitors. *Bioorg Med Chem Lett.* 2006; 16:2170–2172. [PubMed: 16483771]
66. Ribeiro, RdA; De Lores Arnaiz, GR. Nantenine and papaverine differentially modify synaptosomal membrane enzymes. *Phytomedicine.* 2000; 7:313–323. [PubMed: 10969726]
67. Tang H, Wei YB, Zhang C, Ning FX, Qiao W, Huang SL, et al. Synthesis, biological evaluation and molecular modeling of oxoisoaporphine and oxoaporphine derivatives as new dual inhibitors of acetylcholinesterase/butyrylcholinesterase. *Eur J Med Chem.* 2009; 44:2523–2532. [PubMed: 19243862]
68. Hitchcock SA. Blood-brain barrier permeability considerations for CNS-targeted compound library design. *Curr Opin Chem Biol.* 2008; 12:318–323. [PubMed: 18435937]

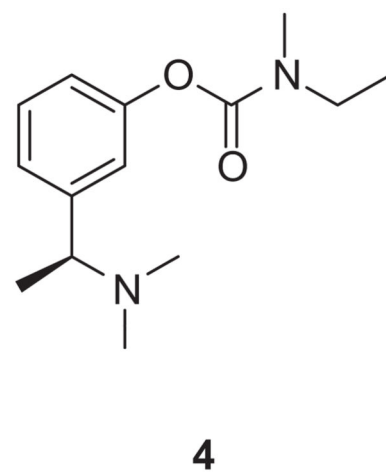
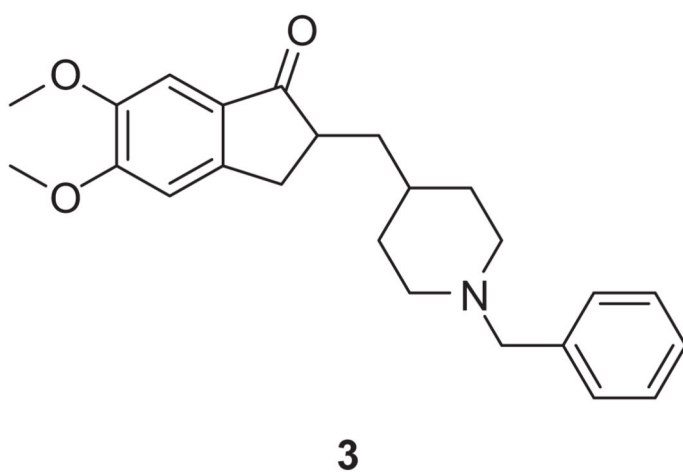
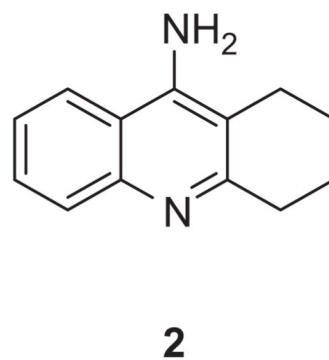
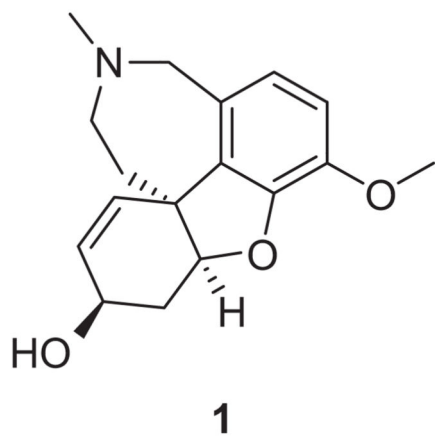


Figure 1.
Clinically available AChE inhibitors.

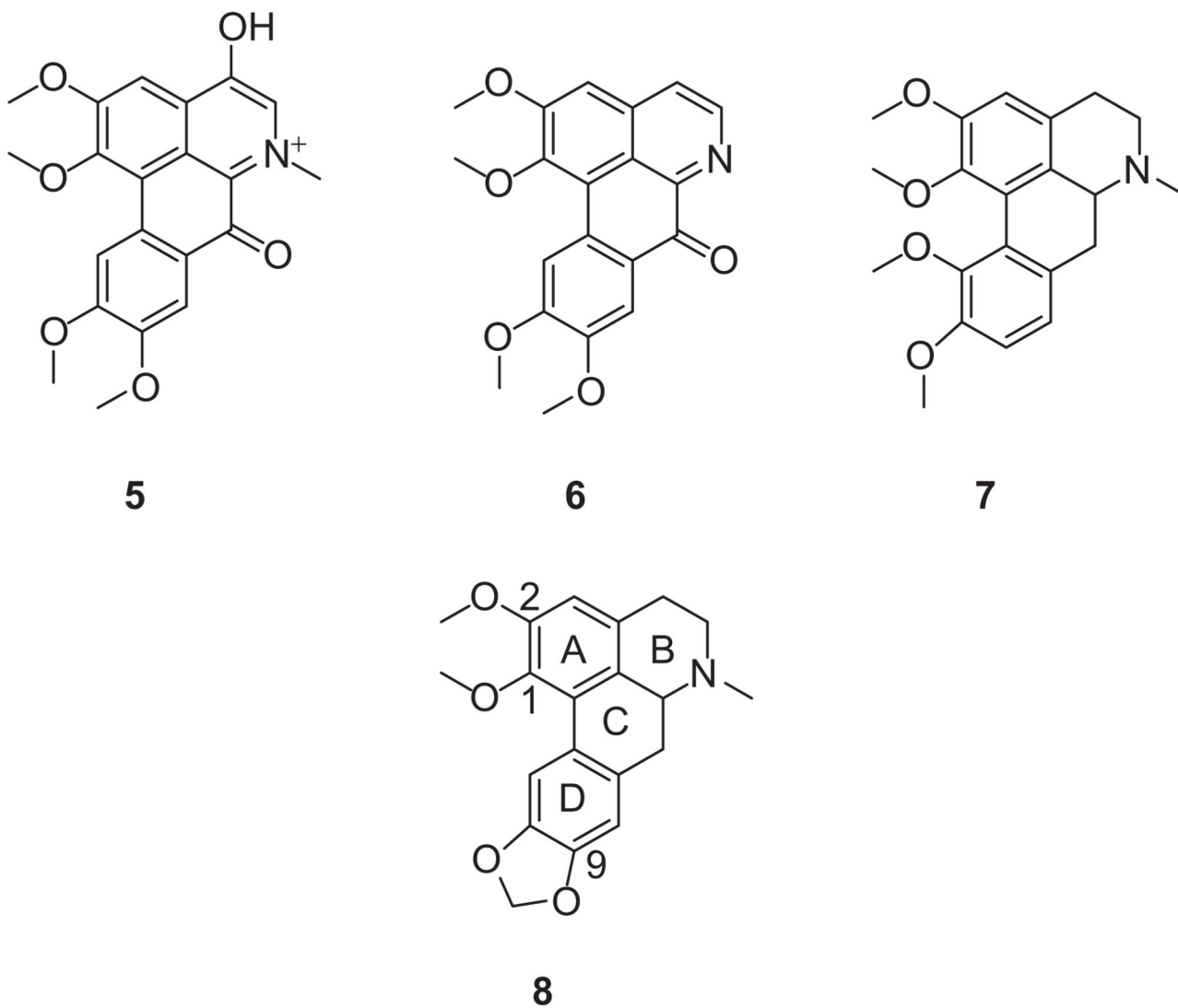


Figure 2.
Structures of known aporphinoid AChE inhibitors (5, 6 and 7) and nantenine (8).

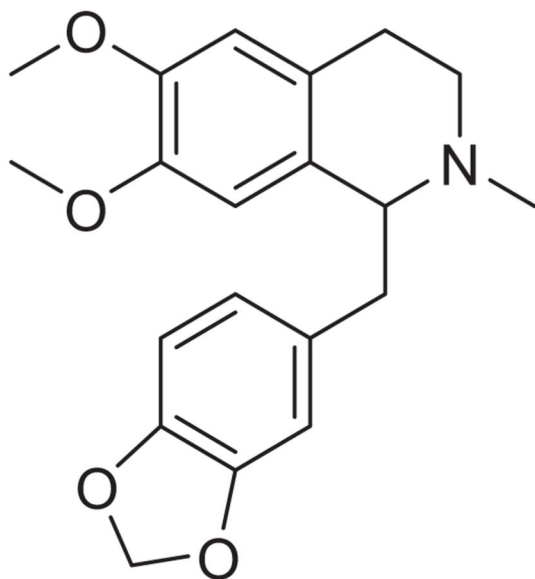
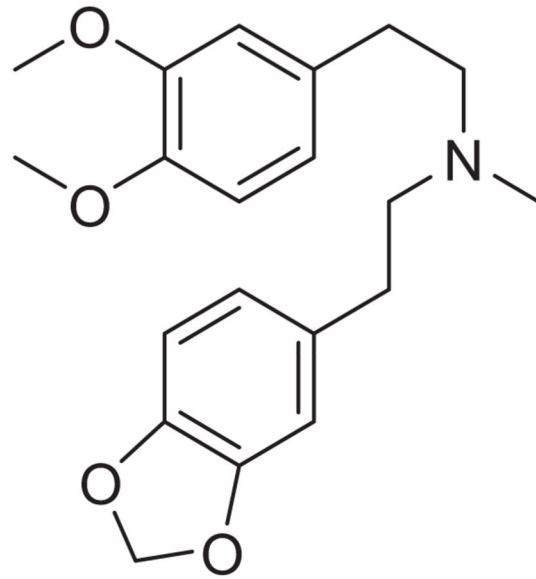
**16****17**

Figure 3.
Other *seco*-ring C nantenine analogs.

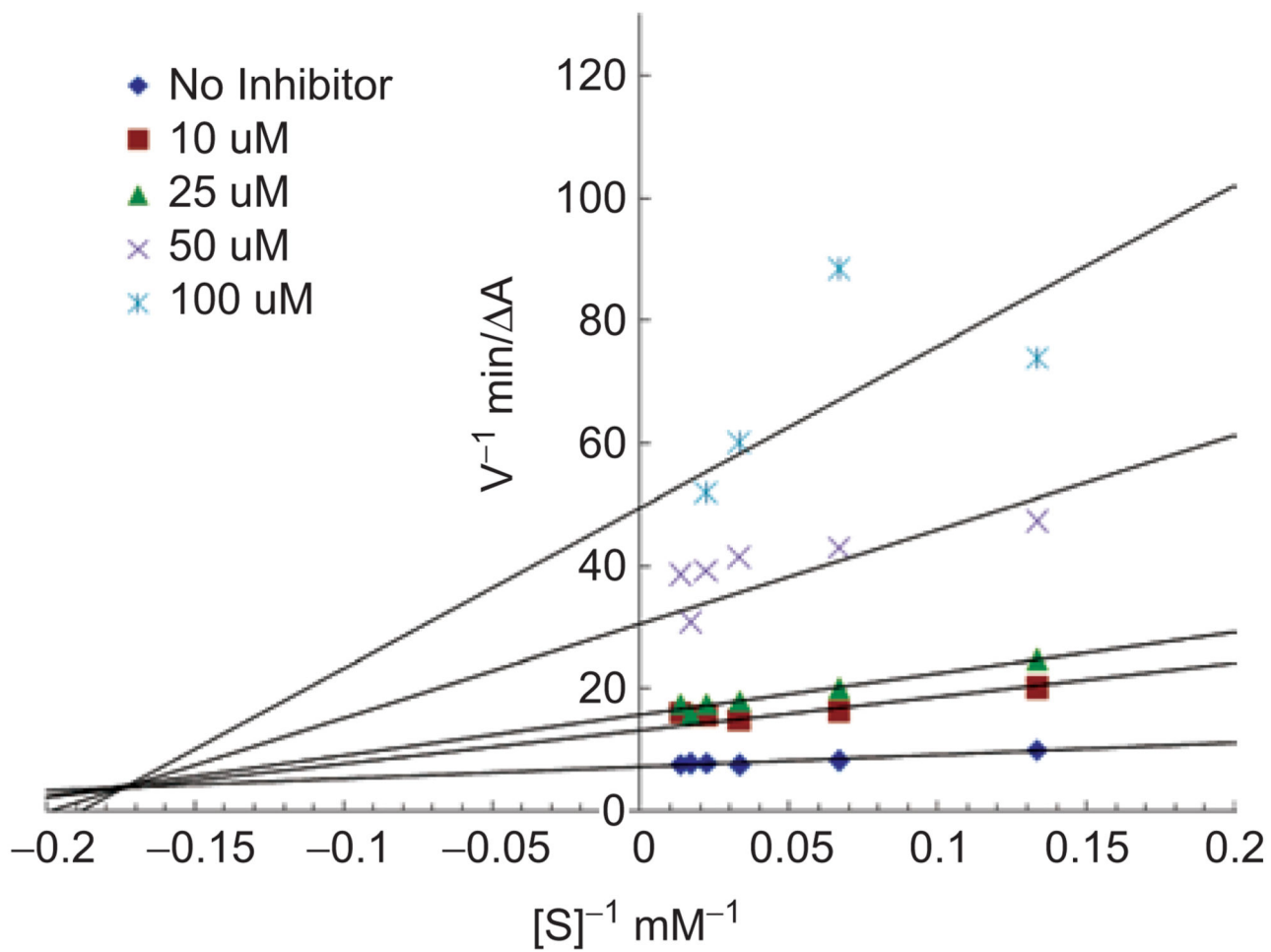


Figure 4. Lineweaver-Burk steady-state inhibition plot showing mixed inhibition for nantenine.

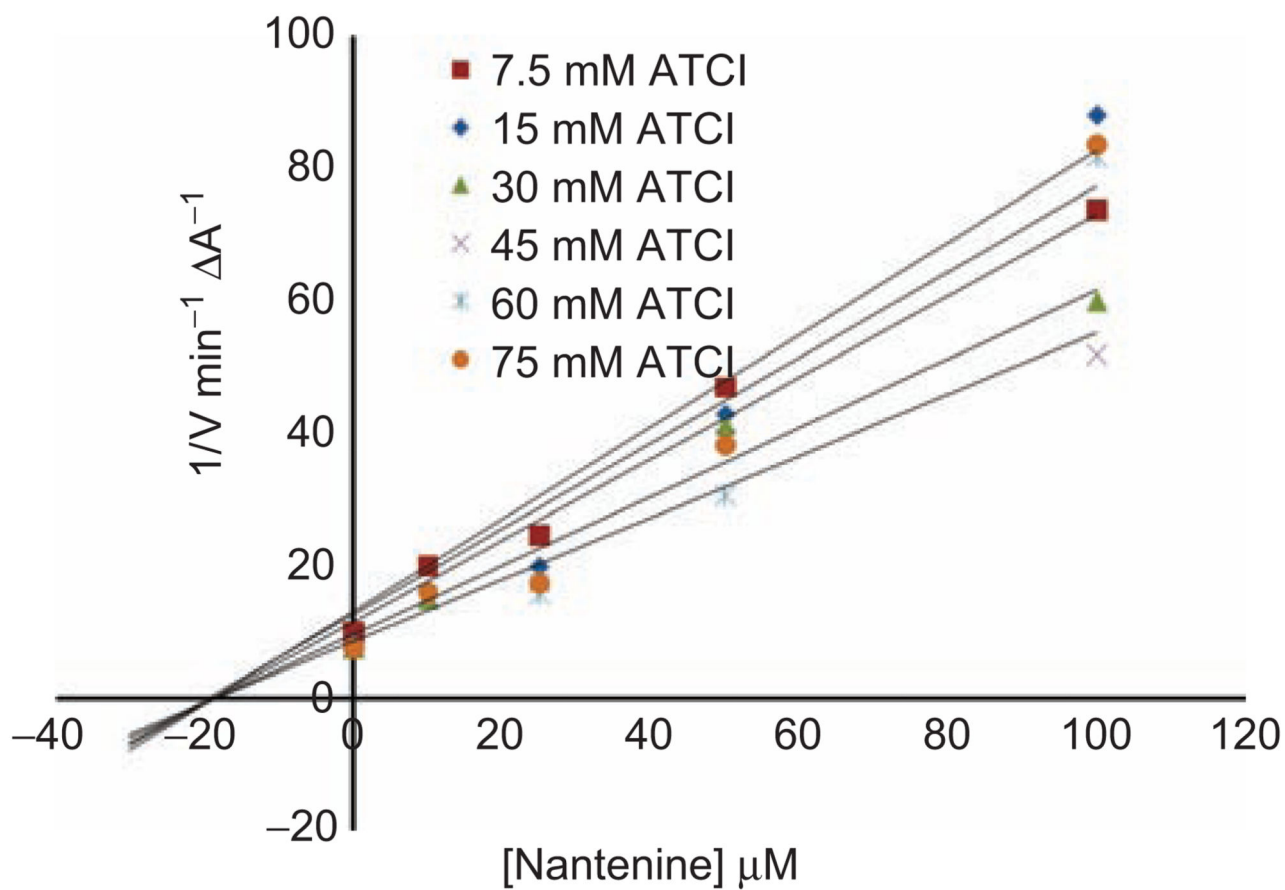


Figure 5.
Dixon plot. (Intercept on the x-axis is $-K_i$).

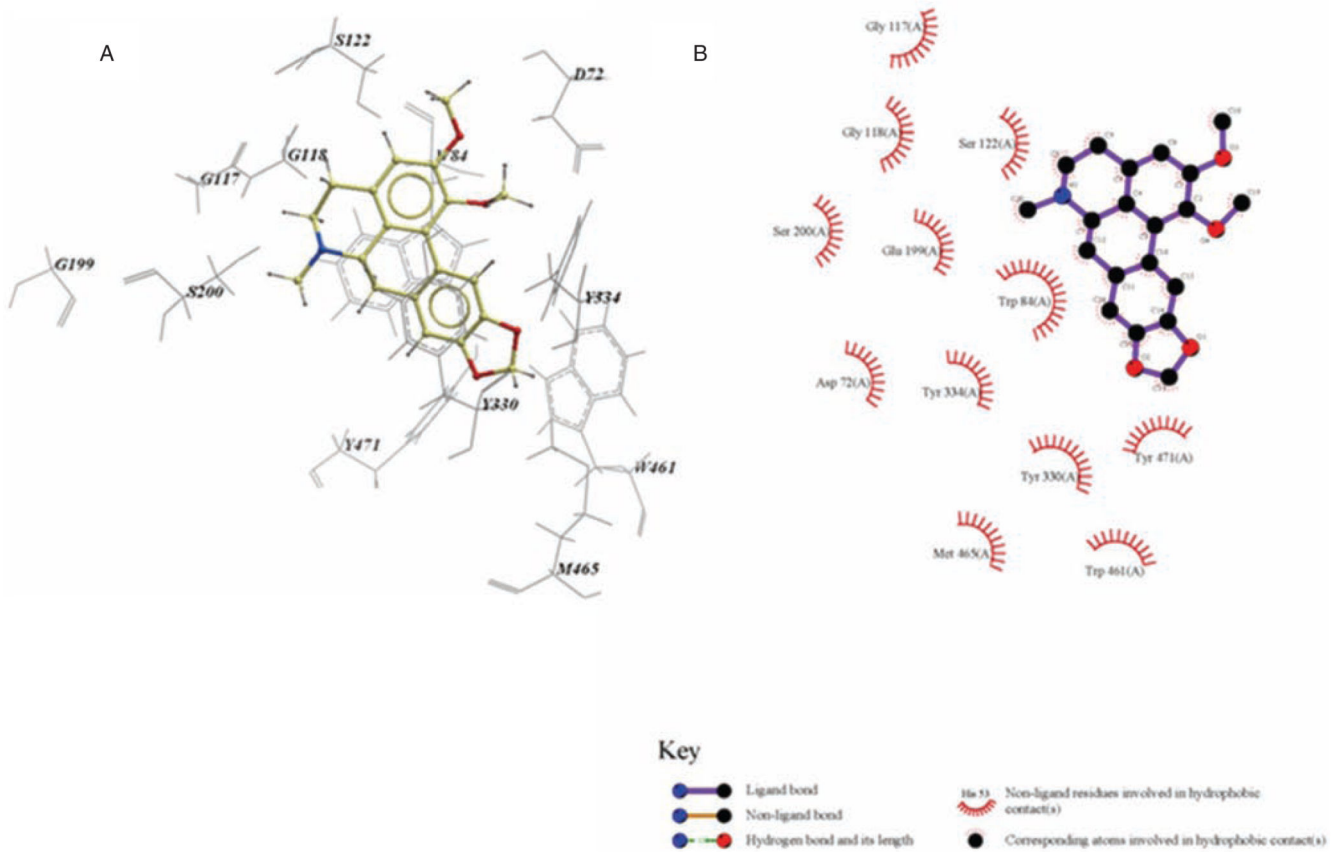


Figure 6.

A is an ICM model of nantenine in the catalytic site of AChE. Pose shown is for lowest energy conformation (pose number 1 in Table 2) and B the LigPlot model of nantenine in the catalytic site of AChE.

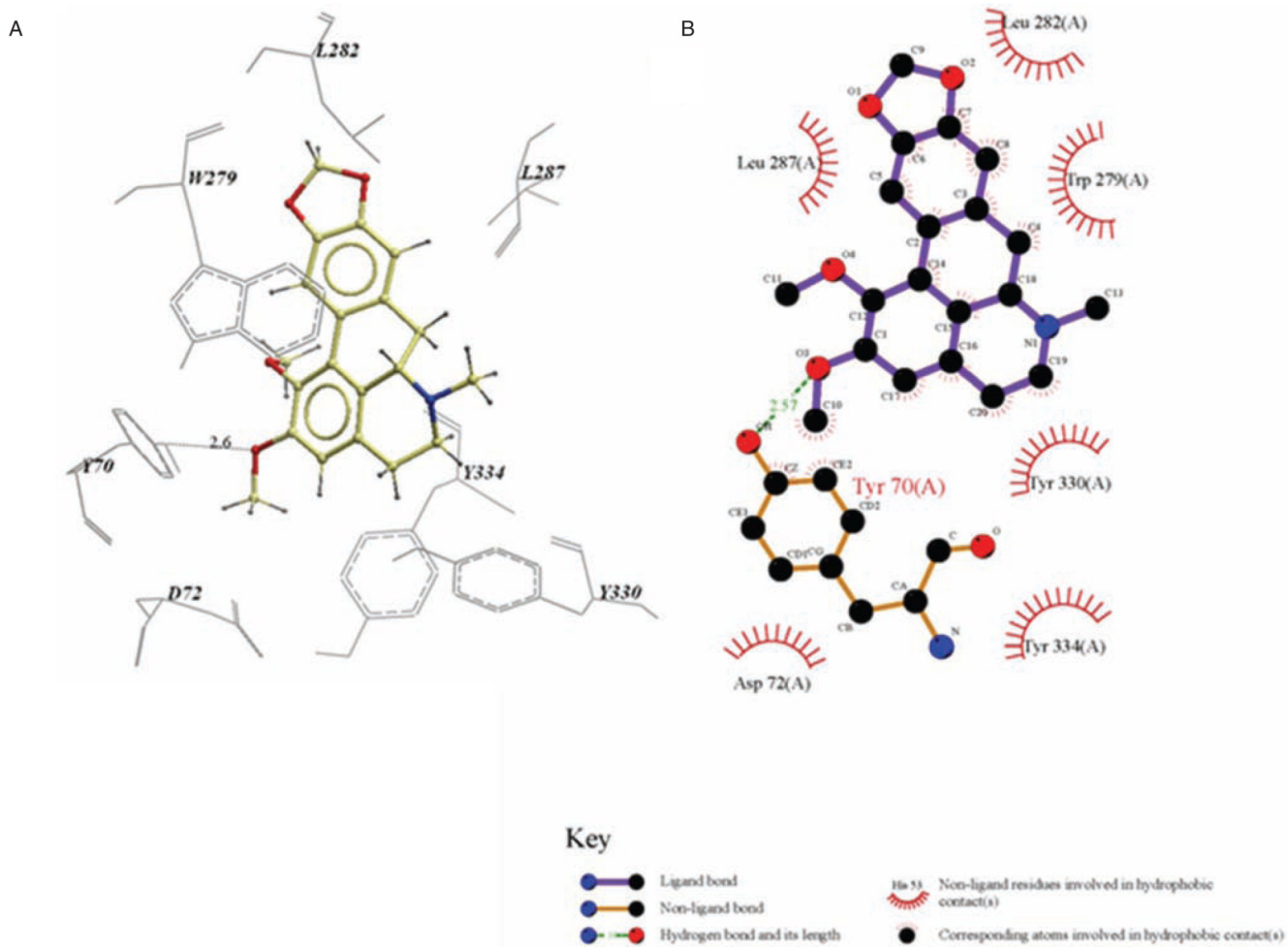
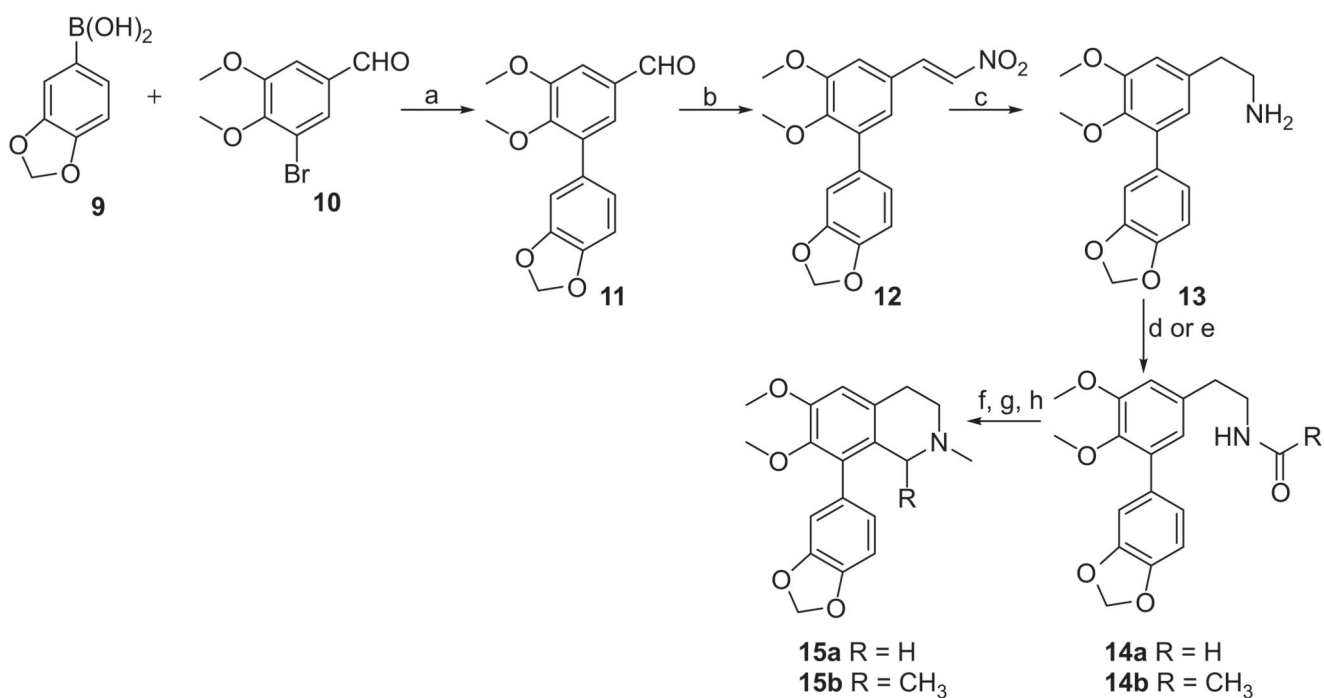


Figure 7.

A is an ICM model of nantenine in the PAS of AChE. Pose shown is for the lowest energy conformation in the PAS (pose number 4 in Table 2) and B is the LigPlot model of Nantenine in the PAS.

**Scheme 1.**

Synthesis of target analogs **15a-15b**. *Reagents and conditions:* (a) Pd(PPh₃)₄, DME, K₂CO₃, reflux, 24h; (b) CH₃NO₂, NH₄OAc, reflux, 4h; (c) LiBH₄, TMSCl, THF, reflux; (d) HCOOEt, Et₃N, DCM for **14a**; (e) acetyl chloride, Et₃N, DCM for **14b**; (f) POCl₃, MeCN, 50°C, 12h; (g) NaBH₄, MeOH, 0°C, 4h; (h) HCNO, NaBH(OAc)₃, DCM, rt, 24h.

Table 1

AChE inhibitory activity of analogues.

| Compound | IC ₅₀ AChE (μM) ^a |
|---------------------------|---|
| Nantenine (8) | 1.09 ± 0.17 |
| 15a | 2.63 ± 0.38 |
| 15b | 2.38 ± 0.21 |
| 16 | 18.06 ± 1.92 |
| 17 | > 100 ^b |
| Galanthamine ^c | 0.53 ± 0.11 |

^aResults are the mean of three replications (± SEM of three experiments).

^bConsidered inactive

^cReference compound.

Author Manuscript

Author Manuscript

Author Manuscript

Author Manuscript

Table 2ICM docking scores for nantenine (**8**) and galanthamine (**1**) in AChE.

| Pose number ^a | ICM docking scores | Binding site |
|--------------------------|---------------------|--------------|
| 1 | -59.2 | Catalytic |
| 2 | -55.09 | Catalytic |
| 3 | -53.9 | Catalytic |
| 4 | -53.75 | PAS |
| 5 | -53.56 | Catalytic |
| 6 | -53.4 | Catalytic |
| 7 | -52.61 | PAS |
| 8 | -52.56 | PAS |
| 9 | -52.31 | PAS |
| 10 | -51.43 | Catalytic |
| Galanthamine | -59.52 ^b | Catalytic |

^a ranked in order of increasing energy

^b top score which corresponds to the lowest energy in ICM

Table 3ICM predicted binding sites for **15a**, **16** and **17**.

| Compound | Pose number | ICM scores | Binding site ^a |
|-------------------------|-------------|------------|---------------------------|
| 15a ^b | 1 | -60.84 | Catalytic |
| | 2 | -57.93 | Catalytic |
| | 3 | -56.9 | Catalytic |
| 16 ^c | 1 | -69.7 | PAS |
| | 2 | -68.14 | Catalytic |
| | 3 | -67.75 | PAS/ Catalytic |
| 17 | 1 | -85.27 | - |
| | 2 | -84.49 | - |
| | 3 | -84.34 | - |

^aCatalytic site or PAS^bTop nine binding poses were in catalytic site, tenth in PAS^cBinding poses four to ten are in PAS

Author Manuscript

Author Manuscript

Author Manuscript

Author Manuscript